Thermochimica Acta 601 (2015) 29–32

Contents lists available at ScienceDirect

Thermochimica Acta

journal homepage: www.elsevier.com/locate/tca

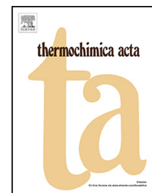

Short communication

Temperature calibration procedure for thin film substrates for thermo-ellipsometric analysis using melting point standards

Emiel J. Kappert, Michiel J.T. Raaijmakers, Wojciech Ogieglo, Arian Nijmeijer, Cindy Huiskes, Nieck E. Benes *

Inorganic Membranes Group, Department of Science and Technology and MESA+ Institute for Nanotechnology, University of Twente, P.O. Box 217, 7500 AE Enschede, The Netherlands

ARTICLE INFO

Article history:
Received 28 October 2014
Received in revised form 2 December 2014
Accepted 16 December 2014
Available online 18 December 2014

Keywords:
Spectroscopic ellipsometry
Temperature calibration
Melting point standards
Thin films
Hot stage

ABSTRACT

Precise and accurate temperature control is pertinent to studying thermally activated processes in thin films. Here, we present a calibration method for the substrate–film interface temperature using spectroscopic ellipsometry. The method is adapted from temperature calibration methods that are well developed for thermogravimetric analysis and differential scanning calorimetry instruments, and is based on probing a transition temperature. Indium, lead, and zinc could be spread on a substrate, and the phase transition of these metals could be detected by a change in the Ψ signal of the ellipsometer. For water, the phase transition could be detected by a loss of signal intensity as a result of light scattering by the ice crystals. The combined approach allowed for construction of a linear calibration curve with an accuracy of 1.3 °C or lower over the full temperature range.

© 2014 Elsevier B.V. All rights reserved.

1. Introduction

Precise control of the sample temperature is essential for studying thermally activated processes [1,2]. Even minor errors in the recorded sample temperature potentially lead to large errors, if derivative calculations on the data are performed [3]. The behavior of thin films may be systematically different from that of bulk materials [4–7]. For the thermal analysis of thin films it is imperative to know the temperature at the substrate–film interface. In such experiments, the properties of the thin film are typically probed by optical techniques, and heating is performed substrate-sided to leave the film open to the light beam. As a result, heat losses may occur from the topside of the sample, or a time-lag may be introduced in the sample heating. The extent of the heat losses can strongly depend on the thickness and thermal conductivity of the substrate. Contrary to the analysis of (semi)bulk samples by, e.g., thermogravimetry or calorimetry [3,8,9], no standardized temperature calibration strategies exist for these type of measurements. In this paper, we will shortly review the existing techniques for probing the temperature of a substrate–film interface. Subsequently, we will demonstrate a simple method to calibrate the substrate–film interface temperature using melting point standards. This simple method is applicable for different types of substrates.

The state-of-the-art temperature calibrations for flat substrates are found in the rapid thermal processing (RTP)-environments in the semiconductor industry, where accurate control over the temperature of silicon wafers is achieved. For these systems, pyrometry is the commonly employed technique. The drawback of this technique is the fact that below ~600 °C lightly-doped wafers are partially transparent at the pyrometer's wavelength [10].

Plainly placing a thermocouple on top of the sample suffers from imperfect thermal bonding [10]. Embedding of a thermocouple or optical sensor into a wafer would circumvent this problem, but is not straightforward [11,12]; moreover, this technique is not generically available for different substrates. Other techniques such as ellipsometry, Raman spectroscopy, or ultrasonic measurements, require knowledge on the change in the (optical) properties of the substrate as function of temperature [10]. Measurement of the thermal changes and matching it to reference data requires extensive knowledge on the technique and the substrate studied.

Precise temperature calibration is a problem that has been extensively addressed in the thermal analysis community. For standard thermal analysis methods, such as thermogravimetric analysis (TG/TGA), differential scanning calorimetry (DSC), and differential thermal analysis (DTA), several temperature calibration methods are available. Typically, calibration involves measuring a transition temperature of a standard, and comparing it with the known value of this transition temperature. The melting point

* Corresponding author. Tel.: +31 53 489 4288.
E-mail address: n.e.benes@utwente.nl (N.E. Benes).

http://dx.doi.org/10.1016/j.tca.2014.12.017
0040-6031/© 2014 Elsevier B.V. All rights reserved.

of metals is typically used for DSC and DTA-capable instruments [1]. This method is also recorded in the current ASTM-standard for DSC calibration [8]. For TG-apparatuses, the state-of-the-art technique involves the placement of a magnet above or under the apparatus, and recording the apparent mass change in a ferromagnetic material when it loses its magnetic properties, as it passes through the Curie temperature [9]. An alternative method involves the use of a dropping weight that hangs from a fusible link made from a melting point temperature standard [13]. Other options include recording the decomposition point of a material [14] or the difference between sample and set temperature that occurs as a result of sample self-heating or cooling (this technique is named calculated DTA and is the technique behind Netzsch's c-DTA®).

The use of melting point standards is an attractive technique for the calibration of wafer temperatures. In the past, this technique has been performed by visual observation of the phase transition [15]. In our experience, visual observations of the phase transition of a thin film are inaccurate because of the small changes in the film properties. Moreover, if a calibration needs to be performed in a closed chamber, visual observation will not be possible.

Here, we report the use of metal melting point standards for simple and fast temperature calibration of thermo-ellipsometric analysis. Because of the light absorbance by the thin metal films, the layers are optically semi-infinite when thicker than ~100 nm, and the substrate can be considered optically invisible. The method relies on the change in the amplitude ratio of the polarized light, Ψ, that takes place upon melting of a thin metal film. Upon heating without a phase change Ψ is relatively constant [16]. Melting induces a step change in Ψ that is a result of an abrupt change in the roughness, the material's density, the films alignment angle or light intensity. The melting temperature of the film is a good indication for the substrate–film interface temperature, because of the large thermal conductivity of the thin metal films. The versatility of the presented method is demonstrated by determining the temperature on silicon wafers and porous alumina substrates.

2. Experimental

In, Sn, Bi, and Zn melting standards (>99.99% purity) were obtained from Netsch. Pb melting standard (99.999% purity) was obtained from Chempur. Silicon wafers ((100)-oriented *p*-type, thickness = 508 μm, front side polished, abbreviated by Si) were obtained from Silchem. Porous α-alumina disks (thickness = 2 mm, $d_{pore} \approx 80$ nm, porosity ≈ 40%) were obtained from Pervatech.

DTA and TGA measurements were carried out on a STA 449 F3 Jupiter (Netsch) fitted with a TGA-DTA-holder (DTA measurement) or a TG-only holder (TGA experiments). Experiments were carried out with ~20 mg of metal, at heating rates of 5–20 °C min^{-1}, under nitrogen. For the TGA measurement, the melting onset was determined using the calculated DTA signal (T_{set}–T_{exp}).

Spectroscopic ellipsometry measurements were recorded on an M2000X spectroscopic ellipsometer (J.A. Woollam) equipped with a heating stage with quartz windows at 70° incident angle (HCS622, INSTEC) and focusing probes. Ψ was measured at an interval of 5 s over the full wavelength range of 210–1000 nm. The measurements were performed under a blanket of nitrogen with negligible flow rate.

To obtain a measurable signal without scattering, a small piece of metal was placed on top of the substrate. Then, the temperature was increased to above the melting point of the metal, and the metal was spread over the surface using a flat spatula. Next, the sample and/or the light beam were aligned to achieve maximum light intensity. The wavelength that displayed the best signal-to-noise ratio was selected for the evaluation of the phase transition. Typically, multiple wavelengths could be selected with identical results. The melting and solidification steps were subsequently studied at different heating rates.

3. Results and discussion

Fig. 1 shows the melting curves of zinc using three different methods. The figure displays a clear difference between the instantaneous melting of the thin film in the ellipsometry, and the time-dependent melting of the metal in the DTA and calculated DTA measurements. Because heating and cooling are both initiated from the wafer–film interface, the absence of hysteresis between the heating and cooling cycle indicates the homogeneous temperature distribution throughout the thin film. The (extrapolated) onset of the curve is the indication for the melting point, as the shape and maximum are heating-rate and sample-mass dependent [1]. As can be expected for a dedicated thermal analysis device, the DTA and TGA measurements displayed the least deviation from the true melting point, with a difference between experimental and known melting temperature of only 0.4 °C for DTA, and a difference of 1.8 °C for TGA (where melting was determined via calculated DTA). For the hot stage of the ellipsometer, a temperature difference of 12.8 °C was determined.

During the ellipsometry measurements, the phase transition fully occurs between two temperature values. The melting points can be determined as the average of these two temperature values, the accuracy of the ellipsometry temperature calibration depends on the data spacing. Shorter measurements intervals therefore lead to a more accurate determination of the melting point; however, at the expense of increased noise in the data, making the transition less pronounced. A measurement time of 5 s was heuristically determined to give optimal results. For the DTA and TGA, the accuracy depends on the precision of the extrapolated onset. Although the onset is theoretically not dependent on heating rate, the extrapolated onset in practice is, and the accuracy can be different for different heating rates.

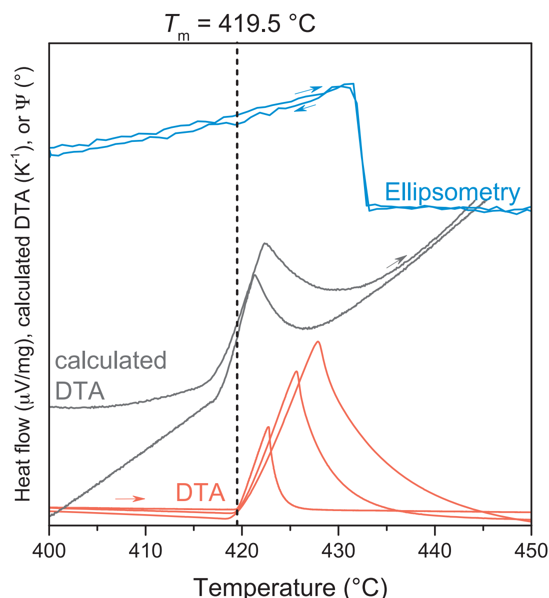

Fig. 1. Melting curves of zinc obtained by DTA, TGA (via calculated DTA), and ellipsometry. For DTA and calculated DTA, the onset of the melting step indicates the melting point. The difference between the known melting point of zinc (419.5 °C) and the recorded melting point indicates the temperature offset that needs to be corrected for.

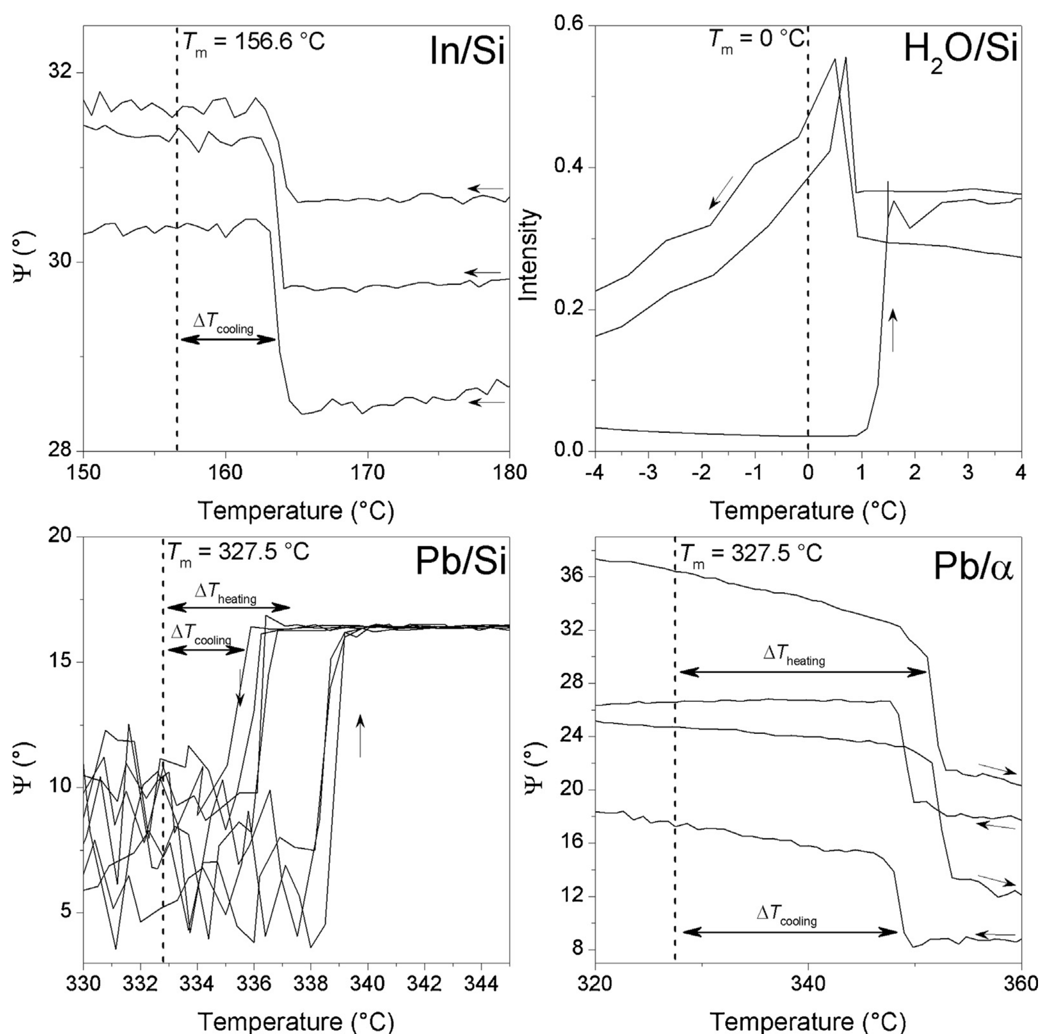

Fig. 2. Melting curves of indium, water, and lead on silicon, and lead on α-alumina, obtained by ellipsometry. The wavelengths at which Ψ was recorded were 500 nm, 300 nm, and 900 nm for In/Si, Pb/Si, and Pb/α-alumina, respectively. For water, freezing leads to the formation of crystals, that scatter all the incoming light, rendering measurements of Ψ impossible. Here, the light intensity was used as an alternative metric. The data demonstrates the accuracy and reproducibility of the melting points, irrespective of noise in the data, or hysteresis in Ψ.

Similar to the data given in Fig. 1, the melting point could be determined for other metals and water. Fig. 2 shows the melting curves of indium, water, and lead on silicon wafers, and that of lead on a porous α-alumina substrate. The melting curves of tin and bismuth were recorded as well. During the experiment these metals showed a strong color change that is indicative for the oxidation of the metal. Some inflow of oxygen during the manual operation of spreading out the metal film over the layer, could not be prevented. Because suitable alternative metals were available, these measurements were discarded.

The melting curves for indium, lead and zinc show a strongly reproducible melting point. Contrary to the results obtained for indium and zinc, a small offset of ~2 °C was detected between heating and cooling cycles for the lead sample. This offset is attributed to the fact that the layer thickness for lead is larger than what could be achieved for indium and zinc, in combination with the lower thermal conductivity of the lead.

For water, upon freezing the ice crystals scatter the incoming light. As a result, the large noise in Ψ prevents the detection of the phase change. However, the scattering upon freezing can be tracked by recording the step change in the light intensity that is detected when freezing occurs. The temperature corresponding to this step change can be used for the temperature calibration. For the metal samples, a step change in the light intensity indicative for the phase transition was found as well. However, determining the onset of melting or solidification from the melting temperature proved to be less accurate. Therefore, for these samples Ψ was chosen as the indicator for the phase change.

The calibration data, such as given in Fig. 2, can be used to construct a calibration curve, see Fig. 3. The proximity of the several data points for one melting point standard demonstrates the precision of the data. Over the full temperature range studied, the deviation between the recorded and actual temperatures follows a linear relation. For the α-alumina substrate, the temperature offsets are higher, as is expected based on the larger sample thickness, lower thermal conductivity of alumina versus silicon, and porosity inside the alumina substrate. Experiments in which a thermocouple was placed onto the silicon wafer, with thermal conductivity paste applied to improve the thermal contact, at 200 °C already resulted in deviations of over 20 °C from the melting point curve.

The accuracy of the calibration curve can be calculated from the 95% confidence interval of the data. Over the whole temperature range, the 95% confidence interval for the silicon wafer temperature is smaller than 1.3 °C, and therefore within the typical limits set for temperature calibration [8]. Because water was not

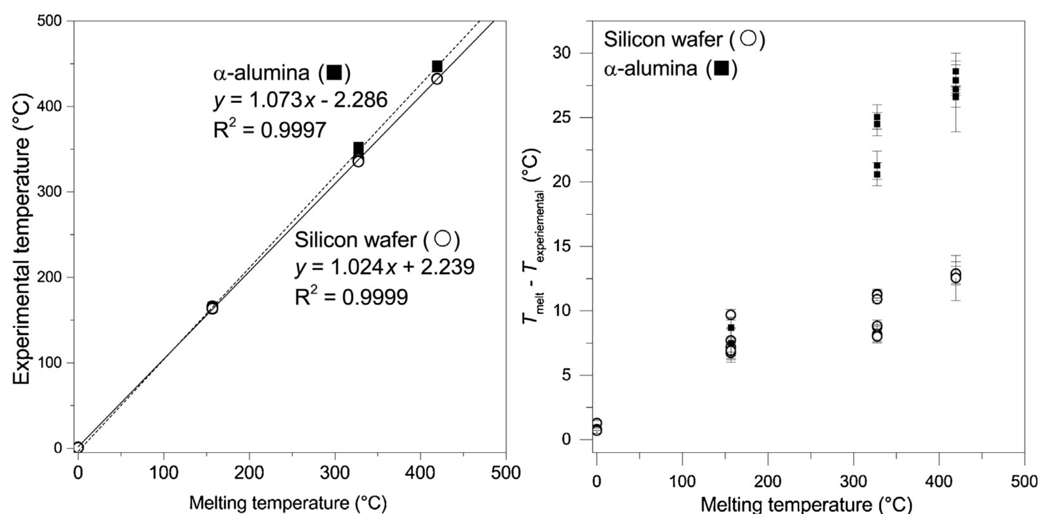

Fig. 3. Calibration curve (left) and deviation between experimentally-determined melting points and literature values (right).

measured for the α-alumina support, the deviations for this support are slightly higher (max 3.3 °C) at lower temperatures. To predict the difference during a single experiment, a prediction interval needs to be constructed. Because of the abundance of measurement data, the maximum deviation for the silicon wafer is within 3 °C over the full temperature range studied.

For all calibration measurements the recorded temperature of the substrate is higher than the known value for the melting point, as a result of heat losses of the sample at the topside. For indium, these heat losses were studied in more detail by performing experiments with different gas flow rates impinging on the sample. The experiments show an increasing difference between the recorded temperature and the theoretical value as a result of the increased cooling of the sample. This difference can be up to 20 °C at flow rates of 0.5 L min^{-1}. More specifically, the melting temperature increased with the square root of the gas flow, thus following the expected trend of the temperature to approximately scale with the gas velocity of the impinging jet [17]. To take into account such temperature variations, temperature calibration is preferably performed in the exact same setting as the actual experiments, i.e., using the same substrate, experimental cell, and flow rates.

4. Conclusions

Temperature calibration of the substrate–film interface was performed by spectroscopic ellipsometry on a sample heated by a hot stage. Indium, lead, and zinc are recommended as melting point standards. The use of tin and bismuth is discouraged due to the strong tendency of these metals to oxidize. Detecting the phase transition using the polarized light beam allows for temperature calibration of a variety of substrates under the experimental conditions, e.g., for the use of gas flows in a purged experimental chamber.

References

[1] S. Vyazovkin, K. Chrissafis, M.L. Di Lorenzo, N. Koga, M. Pijolat, B. Roduit, et al., ICTAC kinetics committee recommendations for collecting experimental thermal analysis data for kinetic computations, Thermochim. Acta 590 (2014) 1–23, doi:http://dx.doi.org/10.1016/j.tca.2014.05.036.

[2] O. Pfohl, T. Hino, J.M. Prausnitz, On the temperature calibration of a thermo-optical apparatus, Fluid Phase Equilib. 112 (1995) 157–162.

[3] S. Vyazovkin, A.K. Burnham, J.M. Criado, L.A. Pérez-Maqueda, C. Popescu, N. Sbirrazzuoli, ICTAC kinetics committee recommendations for performing kinetic computations on thermal analysis data, Thermochim. Acta 520 (2011) 1–19, doi:http://dx.doi.org/10.1016/j.tca.2011.03.034.

[4] Y. Huang, D.R. Paul, Effect of temperature on physical aging of thin glassy polymer films, Macromolecules 38 (2005) 10148–10154, doi:http://dx.doi.org/10.1021/ma051284g.

[5] Z. Fakhraai, J.A. Forrest, Measuring the surface dynamics of glassy polymers, Science 319 (2008) 600–604, doi:http://dx.doi.org/10.1126/science.1151205.

[6] J.L. Keddie, R.A.L. Jones, R.A. Cory, Interface and surface effects on the glass-transition temperature in thin polymer films, Farady Discuss. 98 (1994) 219–230, doi:http://dx.doi.org/10.1039/FD9949800219.

[7] S. Napolitano, M. Wübbenhorst, Structural relaxation and dynamic fragility of freely standing polymer films, Polymer (Guildf) 51 (2010) 5309–5312, doi:http://dx.doi.org/10.1016/j.polymer.2010.09.060.

[8] ASTM Standard E967-08, Standard Test Method for Temperature Calibration of Differential Scanning Calorimeters and Differential Thermal Analyzers (2014) 1–4, http://dx.doi.org/10.1520/E0967-08R14.2.

[9] P.K. Gallagher, R. Blaine, E.L. Charsley, N. Koga, R. Ozao, H. Sato, et al., Magnetic temperature standars for TG, J. Therm. Anal. Calorim. 72 (2003) 1109–1116, doi:http://dx.doi.org/10.1023/A:1025032013135.

[10] P.J. Timans, Rapid thermal processing, in: R. Doering, Y. Nishi (Eds.), Handbook of Semiconductor Manufacturing Technology, CRC Press, Boca Raton, 2008.

[11] W.G. Renken, M.H. Sun, P. Miller, R. Gordon, P.M.N. Vandenabeele, Integrated wafer temperature sensors, US6325536B1 (2001).

[12] T. Iuchi, A. Gogami, Uncertainty of a hybrid surface temperature sensor for silicon wafers and comparison with an embedded thermocouple, Rev. Sci. Instrum. 80 (2009) 126109, doi:http://dx.doi.org/10.1063/1.3274676.

[13] A.R. McGhie, J. Chiu, P.G. Fair, R.L. Blaine, Thermogravimetric apparatus temperature calibration using melting point standards, Thermochim. Acta 67 (1983) 241–250, doi:http://dx.doi.org/10.1016/0040-6031(83)80104-X.

[14] T.L. Slager, F.M. Prozonic, Simple methods for calibrating IR in TGA/IR analyses, Thermochim. Acta 426 (2005) 93–99, doi:http://dx.doi.org/10.1016/j.tca.2004.07.022.

[15] D.S. Fryer, P.F. Nealey, J.J. de Pablo, Thermal probe measurements of the glass transition temperature for ultrathin polymer films as a function of thickness, Macromolecules 33 (2000) 6439–6447.

[16] A.K. Aster, The optical properties of molten metals, Phys. Rev. 20 (1922) 349–357, doi:http://dx.doi.org/10.1103/PhysRev.20.349.

[17] R. Viskanta, Heat transfer to impinging isothermal gas and flame jets, Exp. Therm. Fluid Sci. 6 (1993) 111–134, doi:http://dx.doi.org/10.1016/0894-1777(93)90022-B.